AIP Applied Physics Letters

Thermally switchable adhesions of polystyrene-b lock-poly(n-isopropylacrylamide) copolymer pillar array mimicking climb attitude of geckos

Jem-Kun Chen, Jing-Hong Wang, Jia-Yaw Chang, and Shih-Kang Fan

Citation: Applied Physics Letters **101**, 123701 (2012); doi: 10.1063/1.4754135
View online: http://dx.doi.org/10.1063/1.4754135
View Table of Contents: http://scitation.aip.org/content/aip/journal/apl/101/12?ver=pdfcov
Published by the AIP Publishing

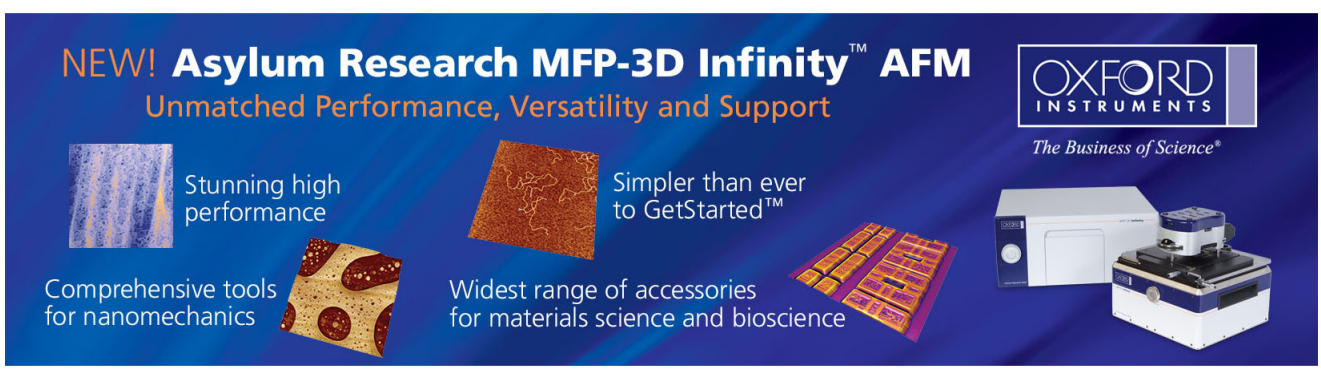

Thermally switchable adhesions of polystyrene-*block*-poly (n-isopropylacrylamide) copolymer pillar array mimicking climb attitude of geckos

Jem-Kun Chen,[1,a)] Jing-Hong Wang,[1] Jia-Yaw Chang,[2] and Shih-Kang Fan[3]
[1]*Department of Materials Science and Engineering, National Taiwan University of Science and Technology, 43, Sec. 4, Keelung Rd, Taipei 106, Taiwan*
[2]*Department of Chemical Engineering, National Taiwan University of Science and Technology, 43, Sec. 4, Keelung Rd, Taipei 106, Taiwan*
[3]*Department of Materials Science and Engineering, National Chiao Tung University, 1001 University Road, Hsinchu 300, Taiwan*

(Received 28 November 2011; accepted 4 September 2012; published online 21 September 2012)

Inspired by the gecko foot pad, we fabricated polystyrene-*block*-poly(*N*-isopropylacrylamide) (PS-*b*-PNIPAAm) copolymer pillar array to mimic climbing attitude of a gecko, alternately attach to and detach from a surface. The pillar array structure of the PS segment significantly enhances both of the hydrophilic and hydrophobic property of PNIPAAm segment tips at 25 and 50 °C, respectively, which could generate alternating adhesive forces of approximately 120 and 11 nN. The dramatic change in adhesive and friction force difference at 25 and 50 °C may guide the design of bio-inspired artificial analogues, which could approach gecko's climbing behavior. © *2012 American Institute of Physics*. [http://dx.doi.org/10.1063/1.4754135]

Geckos and many insects such as flies, beetles, and spiders have extraordinary climbing abilities: They can firmly attach and easily detach from almost any kind of surface (whether hydrophilic or hydrophobic, rough or smooth, dry or wet). The extraordinary ability arises from the tissue on the gecko's foot, which is composed of setae with tips containing spatulas. In the case of small insects and flies, capillary forces have been shown to be responsible for their adhesion. In the case of larger animals such as geckos, the high adhesion and friction have been attributed to van der Waals forces coupled to the complex surface topography of their toes, which are covered with fine regular structures (setae and spatula) with characteristic dimensions and geometries. Bioadhesion has received much experimental and theoretical attention recently[1]—especially that of geckos,[2] the largest animals capable of running on walls and ceilings.[3] The attachment pads of many insects and geckos are covered with long micro- to nanosized hairs with characteristic geometries and mechanical properties. This remarkable surface topography enables these animals to firmly attach to and readily detach from almost any kind of surface. As is evident from Nature, this adhesion concept promises enormous application potential. To date, most detailed investigations have regarded the effects of fibril size for a constant flat punch-like tip shape.[4] Nature provides, however, a variety of contact shapes: spherical, conical, filament-like, flat, toroidal, and concave terminals.[5] Most published reports focused on the significance of geometries in physical systems to pursue high adhesive force, but climbing aptitude of geckos can not be satisfied by this single property of high adhesive force. The investigation generating high and low adhesive forces simultaneously to mimic the climbing aptitude of geckos still has rarely been reported in the design of artificial analogues.

The use of polymers as building blocks for surface modification allows the preparation of "smart" or responsive surfaces that function based on conformational changes in the polymer backbones.[6,7] Stimuli-responsive hydrogels, which undergo large reversible volume changes in response to variations in environmental factors, are excellent candidates for various chemical or biological detection applications.[8,9] Inspired by these structures on the attachment pads of a beetle, fly, spider, and gecko, various kinds of patterned surfaces with large numbers of regular micro- to nanoscale structures, including cylindrical or conical pillars (columns or posts) with flat, spherical, toroidal, or concave ends, have been designed and fabricated.[2,3] Indeed these geometries could generate high adhesive force on the surface, however, a gecko should possess ability of switchable adhesions, which they can climb through a surface. We are unaware, however, of any previous reports included the stimuli-respective property to integrate high and low adhesion on a surface for alternate attachment to and detachment from a surface as that found in Nature. In this context, for this present study, we introduce a stimuli-respective polymer to combine the concepts of geometry to design a biological artificial analogue. Our pillar arrays of block copolymer brushes were prepared from poly(*N*-isopropylacrylamide) (PNIPAAm) on polystyrene (PS) tips through atom-transfer radical polymerization (ATRP).[10,11] Below the lower critical solution temperature (LCST), the PNIPAAm chains are strongly hydrated and possess an extended conformation; when heated above the LCST, however, the polymer undergoes a phase transition to a collapsed morphology, due to dehydration.[12] The thermo-respective behavior of PNIPAAm could be enhanced to generate a dramatic adhesion difference through the PS pillars. Our goal for this paper is to guide the design of bio-inspired artificial analogues by combining geometry and stimuli-respective property to approach climbing attitude of a real gecko more closely.

[a)]Author to whom correspondence should be addressed. E-mail: jkchen@mail.ntust.edu.tw. Tel.: +886-2-27376523. Fax: +886-2-27376544.

Figure 1 outlines our basic strategy for the fabrication of the patterned PS-*b*-PNIPAAm copolymer brushes, using a very-large-scale integration (VLSI) process developed in a previous study.[13] (a) The Si wafer was spin-coated with the photoresist hexamethyldisilazane (HMDS) at a thickness of approximately 780 nm. A contact hole array on the photoresist was then successively patterned using a lithography process. (b) The sample was subjected to oxygen plasma treatment (OPT) to chemically modify the bottom surface.[14] (c) The initiator units were assembled selectively onto the bare regions of the bottom Si surface after OPT. ATRP of the mixture monomer [80 mol. % styrene, 20 mol. % 1,4-divinylbenzene] was performed according to a previously reported method.[10,15] Polymerization of the monomer mixture inside the square hole array of the photoresist generated the pillars as the mimicked setae. (d) The Si–PS surfaces were used as macroinitiators for subsequent surface-initiated ATRP of NIPAAm to produce diblock copolymer brushes. Polymerization was sequentially performed at room temperature inside the square hole array of the photoresist to impart thermally responsive properties to the contact area of each pillar as mimicked spatulas. (e) The remaining photoresist was removed from the PS-*b*-PNIPAAm–grafted Si surface by rinsing with a slightly basic aqueous solution, leaving behind the chemically patterned PS-*b*-PNIPAAm brush surface. We used x-ray photoelectron spectroscopy (XPS) to determine the chemical compositions of the modified Si surfaces and ellipsometry and high-resolution scanning electron microscopy (HR-SEM) to measure the thickness of the copolymer grafts on the Si substrate. We determined the water contact angle (WCA) by fitting a Young–Laplace curve around the drop. Heterogeneous (chemically or geometrically) surfaces typically exhibit contact angle hysteresis; the earliest modeling of liquid drops on rough surface was performed by Wenzel[16] and Cassie.[17] If a liquid fills up the rough surface to form a completely wetted contact with the surface, the system is said to exist in the Wenzel state; if, however, a liquid droplet sits on a composite surface composed of solid and air, it is said to occupy the Cassie state. The contact angle hysteresis ($\Delta\theta$), defined as the difference between the advancing and receding contact angles ($\Delta\theta = \theta_{adv} - \theta_{rec}$), can be used to determine the state of a liquid droplet. If the contact angle hysteresis is small (large), then the droplet exists in the Cassie (Wenzel) state. Thus, the contact angle hysteresis is responsible for the pinning of liquid droplets on a surface.

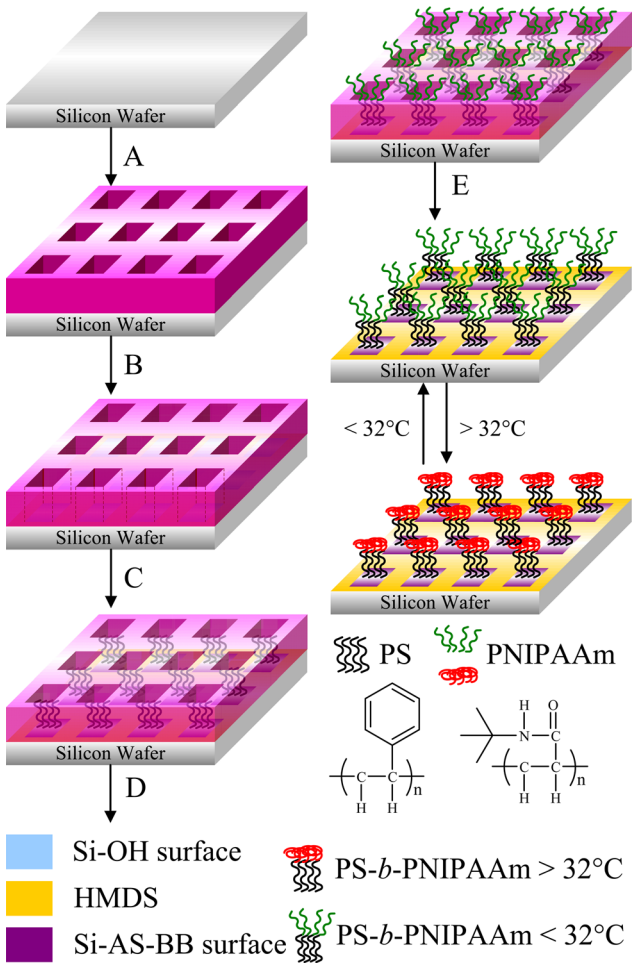

FIG. 1. Schematic representation of the process used to fabricate surfaces chemically micropatterned with PS-*b*-PNIPAAm brushes. (a) Si wafer treated with HMDS in a thermal evaporator. Photoresist spin-coated onto the Si surface presenting $Si(CH_3)_3$ groups. Electron-beam lithography used to pattern the photoresist as hole arrays possessing various aspect and duty ratios on the surface. (b) OPT used to chemically modify the exposed regions presenting $Si(OCH_3)_3$ groups and to convert the topographic photoresist pattern into a chemically modified surface pattern. (c) The initiator units were assembled selectively onto the bare regions of the bottom Si surface after OPT. (d) Sample grafting, through surface-initiated ATRP of a mixture of styrene and 1,4-divinylbenzene (DVB), from the functionalized areas of the patterned initiator to form pillar arrays of cross-linked PS brushes. (e) Object grafting, through surface-initiated ATRP of NIPAAm from the macroinitiator on the top of the pillars, to generate PS-*b*-PNIPAAm copolymer brush pillars. (f) Photoresist removed through treatment with a slightly basic aqueous solution. The pillar arrays of the copolymer brushes on the surface exhibited thermally dependent adhesive properties between 25 and 50 °C.

Our PS-grafted layer had a thickness of 537 nm, which is greater than the value reported elsewhere,[18] presumably because we performed the Si–ATRP of styrene within the square hole array of the photoresist. In addition, the increase in thickness of approximately 223 nm, relative to the initial PS layer, resulted from the formation of PNIPAAm blocks. XPS analysis confirmed the changes in the chemical composition of the Si surface after grafting. Table I summarizes the atomic ratios found at the Si–initiator, Si–PS, and Si–PS-*b*-PNIPAAm surfaces. For the PS-grafted surface, we observed only C atoms, suggesting that the surface was completely covered with a layer of PS. Because the thickness of the grafted PS layer was much greater than the sampling depth (ca. 10 nm) of the XPS system, the N 1s and O 1s components of the initiator were not discernible after the addition of the PS block. Because PNIPAAm comprises C, H, O, and N atoms, we observed the signals of its N 1s and O 1s components after grafting. Static WCA measurements revealed the wettabilities of the functionalized Si surfaces at the various stages, consistent with those from previous studies.[19–21]

TABLE I. Atomic ratios of the Si–initiator, Si–PS, and Si–PS-b-PNIPAAm surfaces, calculated through XPS analysis.

Surface	C/Si	O/Si	N/Si	Br/Si
Si–initiator	0.4	0.4	0.1	0.0
Si–PS	129.1	5.7	4.7	2.3
Si–PS-*b*-PNIPAAm	115.5	28.5	19.3	2.3

After modification with PNIPAAm, the surface exhibited thermoresponsive properties, with WCAs of 41.6° and 82.7° at 25 and 50 °C, respectively. This strong temperature dependence of the surface wettability further confirmed the presence of the PNIPAAm layer of the copolymer.

Atomic force microscopy (AFM) was used to visualize the morphology of pillar arrays of PS-b-PNIPAAm brush. 3D (left), 2D (right), and line cross-section (bottom) analysis AFM topographic images of pillar arrays of PS-b-PNIPAAm brush for 200-nm resolution were depicted in Figure 2(a), revealing that the copolymer brush existed at 25 °C as a dense distinctive overlayer, with pillar diameters of ca. 200 nm, within a scanning area of $10 \times 10\,\mu$m. From line cross-section (bottom) analysis, the PNIPAAm brushes texture with the same height (760 nm) at 50% relative humidity was clearly shown. Each copolymer pillar was fabricated successfully as a cylinder structure with a top diameter of 188 nm and a bottom diameter of 207 nm.[22] A brief rinse (~15 s) in water at 50 °C and subsequent lyophilizing results in conformational change because of deswollen and phase-separated PNIPAAm segment. As a result, after increasing the temperature to 50 °C, however, the pillar diameter increased by approximately 93 nm; that is, thermally responsive behavior was manifested as collapse of the PNIPAAm (Figure 2(b)). Re-immersion into water at 25 °C and subsequent lyophilizing returns to re-hydration of the PNIPAAm and extension of the film to a swelling state. For each pillar, the cylinder structure returns to the original scale after temperature-tuning process.[23] This behavior was reversible over five cycles.

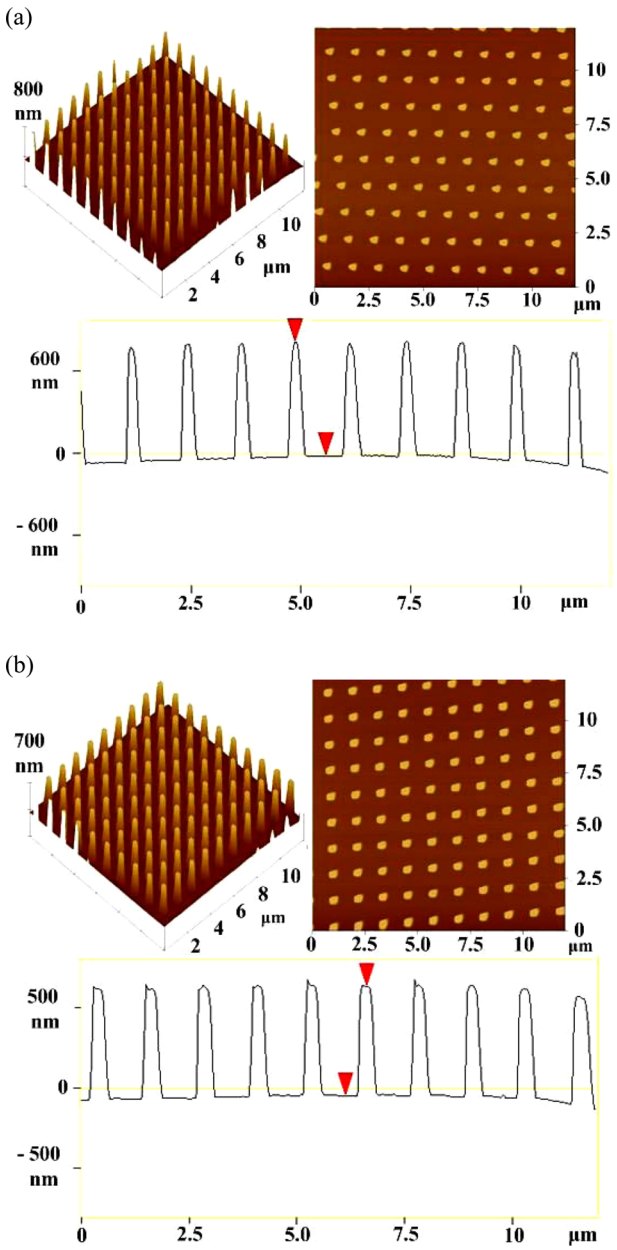

FIG. 2. 3D (left), 2D (right), and line cross-section (bottom) analysis AFM topographic images ($10 \times 10\,\mu$m) of 200-nm resolution pillar array of PS-PNIPAAm copolymer brush at (a) 25 and (b) 50 °C.

Figure 3(a) reveals that the WCAs of the Si–PS on both the flat and pillar surfaces remained static at 25 and 50 °C. After block copolymerization with PNIPAAm, however, the PS-*b*-PNIPAAm copolymer brushes exhibited higher WCAs at 50 °C than they did at 25 °C as a result of the presence of the more-hydrophobic PNIPAAm segments, consistent with other reports.[24] Here, we define the static WCA difference at 25 and 50 °C as a thermal-responsive efficiency ($\Delta\theta_{eff} = WCA_{50\,^\circ C} - WCA_{25\,^\circ C}$) during the phase transition. The value of $\Delta\theta_{eff}$ of

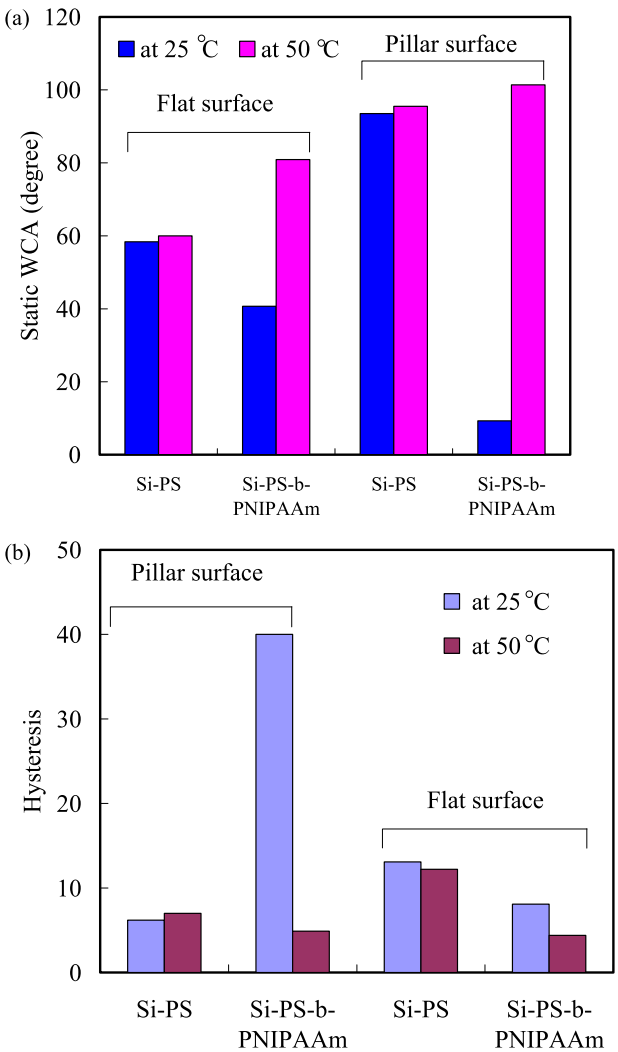

FIG. 3. (a) Static WCAs of flat and pillar arrays of Si–PS and Si–PS-*b*-PNIPAAm surfaces at 25 and 50 °C. (b) Variation of the WCA hysteresis, calculated from the advancing and receding WCAs of droplets, on flat and pillar array of Si–PS and Si–PS-*b*-PNIPAAm surfaces at 25 and 50 °C.

the PS-*b*-PNIPAAm pillar array was higher than that of the flat surface because of capillary and meniscus forces.[25] Furthermore, we recorded the dynamic WCAs (advancing and receding contact angles) on the pillar structure surfaces to determine their hysteresis at 25 and 50 °C, respectively. A discontinuity in the hysteresis exists when a transition occurs between the Wenzel and Cassie states. In our case, a liquid droplet on a composite surface is composed of solid and air. At 25 °C, the PS-*b*-PNIPAAm pillar array existed in the Wenzel state because of higher hysteresis (Figure 3(b)); the system resided in the Cassie state at 50 °C because of lower hysteresis. Thus, a transition occurred between the Wenzel and Cassie states during temperature tuning. In the absence of the pillar structure, the hysteresis remained almost constant at 25 and 50 °C. Thermally responsive properties resulted after copolymer grafting because the PNIPAAm blocks feature terminal groups that are thermally responsive, thereby generating switching properties in terms of the contact mode (Wenzel or Cassie state).

The geometry of the adhesion tests with a representative experimental force−distance curve obtained on patterned surfaces with pillars of Si-PS-b-PNIPAAm along 80 μm of scanning distance is depicted in pervious report.[23] During loading, the curves initially show a nonlinear response related to the change in the stiffness as the number of pillars in contact increased. No significant approach-retraction hysteresis could be noticed, indicating that the deformation of the sample is predominantly elastic, and viscoelastic effects, while present, can be neglected. The final detachment event gives the value of the adhesive force. The influence of the fabrication procedure, the environmental conditions (temperature and humidity), and the experimental parameters (indentation rate and preload) on the adhesion results were first tested and later carefully controlled to allow meaningful comparison of data obtained from different specimens. Changes in humidity can also influence the experimental adhesive force, as liquid bridges around the contact areas result in higher adhesion. Meniscus forces on patterned surfaces depend on the geometry and radius of the contact surfaces, the hydrophobicity of the materials.[25] Adhesion is generally obtained by the amount of force necessary to separate two surfaces in contact and the results. We observed that the adhesive forces were closely related to the pillar structure of the PS-*b*-PNIPAAm brushes, but they were also influenced strongly by the thermally responsive properties of the PNIPAAm blocks, as revealed in Figure 4(a). Adhesion force friction also follows a similar trend to the SWCA data at 25 and 50 °C. In addition, the adhesive force difference at 25 and 50 °C, respectively, on the PS-*b*-PNIPAAm pillars increased gradually upon increasing the pillar resolution. Compared with the biological system,[3] higher resolution pillar array approaches more closely geometries of hair-like structure in bio-attachment pad, such as fly, spider, and gecko, leading to enhancement of adhesion force difference during temperature-tuning process. The adhesion of the copolymer pillars at 25 °C exhibits larger than that of bio-attachment pad, such as fly, spider, and gecko (40 nN), suggesting that the copolymer pillars may attach on a surface firmly.[3,5] In addition, the adhesive force is below 15 nN at 50 °C to detach from a surface facilely. The alternately

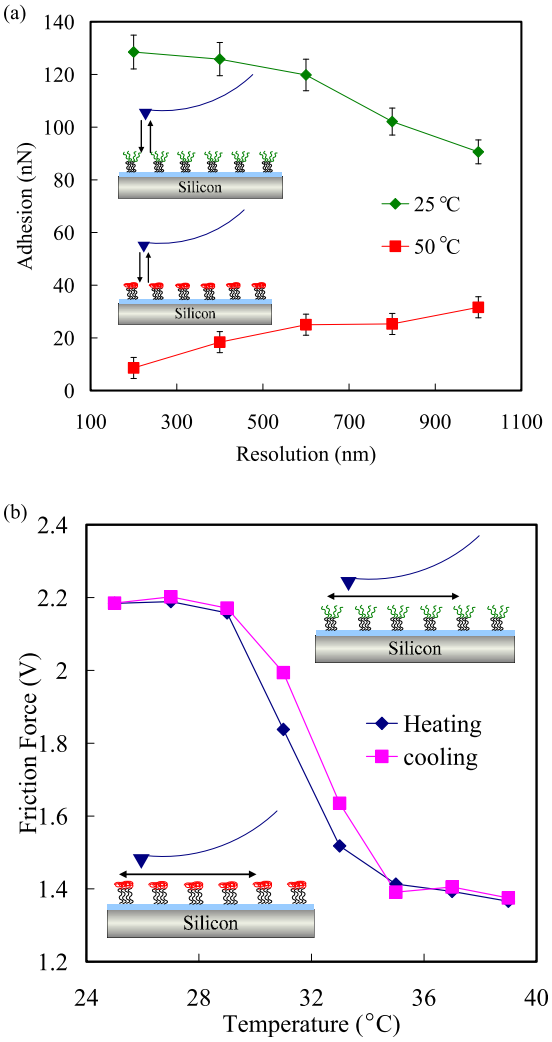

FIG. 4. (a) Changes in adhesive forces of the tethered PS-*b*-PNIPAAm pillars plotted as a function of resolutions. Insets: Illustrations of an AFM tip alternately attaching to and detaching from the copolymer pillar to observe the transitions of the terminus from brush to globule structures at 25 and 50 °C. (b) Dependence of the friction force under a normal load of 200 nN on 200 nm-resolution copolymer pillar array with temperature. Insets: Illustrations of an AFM tip alternately scraping the copolymer pillar to observe the transitions of the terminus from brush to globule structures at 25 and 50 °C.

switchable adhesive force fulfills the climbing attitude of a real biological system more closely. The two insets to Figure 4(a) illustrate AFM tips alternately attaching to and detaching from the copolymer pillar array surface with terminal transitions from brushes to globules at 25 and 50 °C, respectively. Compared with the flat PS-*b*-PNIPAAm surface, the copolymer surface featuring the pillar arrays exhibited a significant enhancement. This thermal switching of the adhesive force of the copolymer brush pillars was reversible for at least four cycles, whereas that of the flat surface of PS-*b*-PNIPAAm copolymer brushes was barely evident.

Furthermore, we measured the friction force on the 200 nm-resolution copolymer pillar surface with temperature under a normal load of 200 nN by AFM/friction force microscopy (FFM). The friction force is given here in the form of voltage signal, which is proportional to the real friction force.[26] The results from various surfaces could be compared to each other. As seen in Figure 4(b), the friction force on the PS-*b*-PNIPAAm pillars decreased abruptly at ca. 32 °C,

corresponding to the LCST of PNIPAAm segment. The real area of contact and surface chemistry affects friction force at nanoscale in dry/wet contacts strongly.[26] The real area of contact is dependent upon the area density and height of nanopillars. With the same tip scan velocity, increasing of fractional surface coverage, the number of asperities in contact is reduced greatly which lead to the real area of contact reduced and so lead to low friction force. Then, if the surface is hydrophilic, it is easy to form capillary meniscus by them or the adsorbed water molecules, which would lead to large shearing strength and higher friction.[27] In other words, if the surface is hydrophobic, it would get the opposite result. The contact regime of PNIPAAm made the surface more hydrophilic and hydrophobic which lead to higher and lower surface energy at 25 and 50 °C, respectively, so 200 nm-resolution copolymer pillars showed the largest difference of friction force between 25 and 50 °C in this study.

Different to other reports focused on geometry for biomimic surface to pursue solely high adhesion, we integrate surface geometry and stimuli-responsive hydrogel tips to generate dramatic change in adhesion and friction force at 25 and 50 °C, respectively. We believe that the involving stimuli-respective property in fine regular structures (setae and spatula) with characteristic dimensions may approach a biological system more closely in climbing aptitude. We intend to employ this processing strategy to create biomimetic versions of gecko's foot pads, with the ability to alternately attach to and detach from, and thereby climb up, a surface. The results show that thermally switchable performance of the copolymer pillars on adhesion could be apparently enhanced. It is expected that this paper could provide additional insight on the biomimetic foot pad by tailoring the surface topography and using stimuli-responsive hydrogels as the contact regime.

We thank the National Science Council of the Republic of China for supporting this research financially.

[1]K. Autumn, Y. A. Liang, S. T. Hsieh, W. Zesch, W. P. Chan, T. W. Kenny, R. Fearing, and R. J. Full, Nature **405**, 681–685 (2000).
[2]A. del Campo, C. Greiner, I. Alvarez, and E. Arzt, Adv. Mater. **19**, 1973–1977 (2007).
[3]E. Arzt, S. Gorb, and R. Spolenak, Proc. Natl. Acad. Sci. U.S.A. **100**, 10603–10606 (2003).
[4]H. Zeng, N. Pesika, Y. Tian, B. Zhao, Y. Chen, M. Tirrell, K. L. Turner, and J. N. Israelachvili, Langmuir **25**, 7486–7495 (2009).
[5]H. Lee, B. P. Lee, and P. B. Messersmith, Nature **448**, 338–342 (2007).
[6]J.-K. Chen, B.-J. Bai, and F.-C. Chang, Appl. Phys. Lett. **99**, 013701 (2011).
[7]J. K. Chen and A. L. Zhuang, Colloid Polym. Sci. **289**, 1283–1294 (2011).
[8]N. A. Peppas, J. Z. Hilt, A. Khademhosseini, and R. Langer, Adv. Mater. **18**, 1345–1360 (2006).
[9]C. H. Chan, J. K. Chen, and F. C. Chang, Sens. Actuators, B **133**, 327–332 (2008).
[10]J.-K. Chen, C.-Y. Hsieh, C.-F. Huang, and P.-M. Li, J. Colloid Interface Sci. **338**, 428–434 (2009).
[11]T.-Y. Chen and J.-K. Chen, Colloid Polym. Sci. **289**, 433–445 (2011).
[12]J.-K. Chen and J.-Y. Li, Sens. Actuators, B **150**, 314–320 (2010).
[13]J.-K. Chen, Z.-Y. Chen, H.-C. Lin, P.-D. Hong, and F.-C. Chang, ACS Appl. Mater. Interfaces **1**, 1525–1532 (2009).
[14]J. K. Chen and T.-Y. Chen, J. Colloid Interface Sci. **355**, 359–367 (2011).
[15]G. Li, J. Fan, R. Jiang, and Y. Gao, Chem. Mater. **16**, 1835–1837 (2004).
[16]R. N. Wenzel, Ind. Eng. Chem. **28**, 988 (1936).
[17]A. B. D. Cassie, and S. Baxter, Trans. Faraday Soc. **40**, 546 (1944).
[18]J. K. Chen and A.-L. Zhuang, J. Phys. Chem. C **114**, 11801–11809 (2010).
[19]J. K. Chen, C. Y. Hsieh, C. F. Huang, P. M. Li, S. W. Kuo, and F. C. Chang, Macromolecules **41**, 8729–8736 (2008).
[20]W. Zhao, L. Wang, and Q. Xue, ACS Appl. Mater. Interfaces **2**, 788–794 (2010).
[21]J.-K. Chen, B.-J. Bai, and F.-C. Chang, J. Phys. Chem. C **115**, 21341–21350 (2011).
[22]H. Tu, C. E. Heitzman, and P. V. Braun, Langmuir **20**, 8313–8320 (2004).
[23]J.-K. Chen, J.-H. Wang, S.-K. Fan, and J.-Y. Chang, J. Phys. Chem. C **116**, 6980–6992 (2012).
[24]L. Li, Y. Zhu, B. Li, and C. Gao, Langmuir **24**, 13632–13639 (2008).
[25]Y. F. Mo, W. J. Zhao, D. M. Huang, F. Zhao, and M. W. Bai, Ultramicroscopy **109**, 247–252 (2009).
[26]S. Y. Song, S. L. Ren, J. Q. Wang, S. R. Yang, and J. Y. Zhang, Langmuir **22**, 6010–6015 (2006).
[27]W. J. Zhao, M. Zhu, Y. F. Mo, and M. W. Bai, Colloids. Surf. A **332**, 78–82 (2009).